Theory of the $d^{10}-d^{10}$ Closed-Shell Attraction: 2. Long-Distance Behaviour and Nonadditive Effects in Dimers and Trimers of Type $[(X\text{-}Au\text{-}L)_n]$ ($n = 2, 3$; X = Cl, I, H; L = PH_3, PMe_3, -N≡CH)**

Pekka Pyykkö* and Fernando Mendizabal

Abstract: We study the nature of the aurophilic attraction (Au^I-Au^I) at its long-range limit for the model systems $[(X\text{-}Au\text{-}L)_n]$ ($n = 2, 3$; X = Cl, I, L = PH_3, PMe_3; X = H, L = -N≡CH) at the ab initio MP2 and Hartree–Fock levels. The nature of the interactions and nonadditive effects at various orientations are related to simple electrostatic induction and dispersion expressions involving the individual properties of each monomer.

Keywords
ab initio calculations · closed-shell attraction · gold · long-range interactions · relativistic effects

Introduction

The experimental and theoretical results available[1–5] for gold(I) complexes show the presence of a weak metal–metal interaction, called aurophilic attraction. The intra- and intermolecular Au^I-Au^I contacts are found in the solid state of the compounds, and they may even govern the supramolecular structure of certain materials.[6]

The supramolecular aggregates in gold(I) complexes of type [X-Au-L] (X = halide or pseudohalide, L = donor ligand) have a varied structural chemistry, from dimers to oligomers and polymers.[7–13] The intermolecular gold–gold contacts between [X-Au-L] complexes typically occur perpendicular to the main molecular axis. The dihedral angle can vary, corresponding to having the monomers in parallel (C_{2v}), antiparallel (C_{2h}) or perpendicular (C_2) orientations (Figure 1). The gold–gold contacts are typically 300–350 pm, associated with a bond energy of the order of 21–42 $kJ\,mol^{-1}$.[14, 15] These parameters depend on several factors, including the nature of the ligands (chemical effects).

From a theoretical point of view, the aurophilic attraction is interesting, because the classical theory of chemical bonding does not give a satisfactory explanation for this type of metal–metal interaction.[16, 17] Only when considered as a correlation effect, strengthened by relativistic effects,[3–5] can this phenomenon be accounted for by theoretical studies.[18, 19]

The intermolecular interactions in general can be analysed in terms of electrostatic, induction and dispersion terms, and short-range Pauli repulsion.[6, 20] The electrostatic terms comprise interactions between the charges or the higher electrostatic multipole moments. The induction terms describe the interactions between these moments and the static polarizabilities α_L. The dispersion terms occur between the frequency-dependent polarizabilities, $\alpha_L(\omega)$, of the monomers.

In Part 2 of this study (Part 1[21]) we try to single out the dominant contributions to the aurophilic attraction by considering the long-range limits for both dimers and trimers of the previously employed [XAuL] monomers at typical geometries. More specifically, the intermolecular interaction energy of dimers and trimers $[(X\text{-}Au\text{-}L)_n]$ ($n = 2, 3$; X = Cl, I, L = PH_3, PMe_3; X = H, L = -NCH) are considered at MP2 and Hartree–Fock levels, and the nature of their interactions are related to

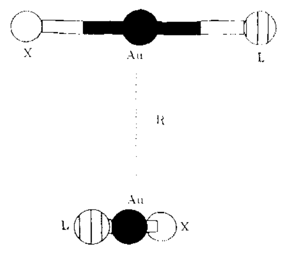

(a) C_2 Symmetry

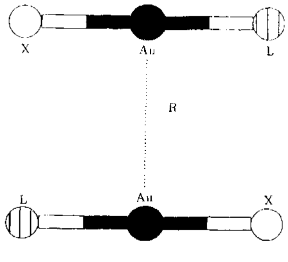

(b) C_{2h} Symmetry

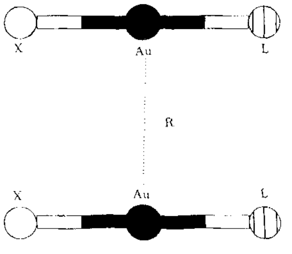

(c) C_{2v} Symmetry

Figure 1. a) Perpendicular (C_2), b) antiparallel (C_{2h}) and c) parallel (C_{2v}) orientations of dimers $[(XAuL)_2]$.

---

[*] P. Pyykkö, F. Mendizabal[+]
Department of Chemistry, University of Helsinki
P. O. B. 55 (A. I. Virtasen aukio 1), FIN-00014 Helsinki (Finland)
Fax: Int. code +(9)191-40169
e-mail: pekka.pyykko@helsinki.fi

[+] On leave of absence from The Department of Chemistry
Faculty of Science, University of Chile (Chile)

[**] Theory of the $d^{10}-d^{10}$ Closed-Shell Attraction, Part 2. Part 1: previous paper.

monomer properties at the specific orientations. For the first time we consider both additive and nonadditive induction terms. As emphasized by Chalasiński and Szcześniak,[22] the dominant nonadditive contributions between polar monomers are $\mu^A \alpha^B \mu^C$, where μ^A is the dipolar moment of monomer A.

Computational Details and Theory

Quantum Chemical Methods: The Gaussian 94 package was used.[23] The basis sets and pseudopotentials (PP) used in the production runs are given in Table 1. The 19 valence electron (VE) quasirelativistic (QR) pseudopotential (PP) of Andrae[24] was employed for gold. We used two f-type polarization functions for gold. This is desirable for a correct description of the interaction energy.[21]

The atoms C, N, P, Cl and I were also treated by Stuttgart pseudopotentials,[25] including only the valence electrons for each atom. For these atoms, double-zeta basis sets of ref. [25] were used, augmented by d-type polarization functions.[26] For the H atom, double-zeta plus one p-type polarization function was used[27] (see Table 1).

Table 1. Basis sets and pseudopotentials (PPs) used in the present work.

Atom	PP	Basis	Remarks
H	–	(4s 1p)/[2s 1p]	$\alpha_p = 0.8$
C	Bergner [25]	(4s 4p 1d)/[2s 2p 1d]	$\alpha_p = 0.1561$, $a_d = 0.80$
N	Bergner [25]	(4s 4p 1d)/[2s 2p 1d]	$\alpha_p = 0.222$, $\alpha_d = 0.864$
P	Bergner [25]	(4s 4p 1d)/[2s 2p 1d]	$\alpha_p = 0.084$, $\alpha_d = 0.34$
F	Bergner [25]	(4s 4p 1d)/[2s 2p 1d]	$\alpha_p = 0.0848$, $\alpha_d = 1.496$
Cl	Bergner [25]	(4s 4p 1d)/[2s 2p 1d]	$\alpha_p = 0.0154$, $\alpha_d = 0.514$
I	Bergner [25]	(4s 4p 1d)/[2s 2p 1d]	$\alpha_p = 0.0326$, $\alpha_d = 0.266$
Au	Andrae [24]	(8s 6p 5d 2f)/[6s 5p 3d 2f]	$\alpha_f = 0.2$, 1.19

We first fully optimized the geometries for the [XAuPR$_3$] (X = Cl and R = H, Me; X = I and R = H) and [HAuNCH] monomers at MP2 level. These geometries were left unchanged when studying the Au^I–Au^I intermolecular interactions in dimers and trimers. These monomer data are given Table 2.

Table 2. Optimized geometries for the [XAuL] monomers at MP2 level. Distances in pm; energy in au.

System	P–H	L–Au	Au–X	HPAu	E
[ClAuPH$_3$]	141.3	224.3	226.3	117.4	–158.47013 [a]
[ClAuPMe$_3$]	–	224.3	227.5	–	–178.94969 [a]
[IAuPH$_3$]	141.4	226.9	255.9	117.6	–154.87424 [a]
[HAuNCH]	–	209.8	153.4	–	–151.93550 [a]

[a] Part 1 [21].

The interaction energies of the dimers and trimers were obtained as Equations (1) and (2), respectively; a counterpoise correction for the basis-set

$$\Delta E = E_{\mathrm{AB}}^{(AB)} - E_{\mathrm{A}}^{(AB)} - E_{\mathrm{B}}^{(AB)} = V(R) \qquad (1)$$

$$\Delta E(\mathrm{MP2}) = E_{\mathrm{ABC}}^{(ABC)} - E_{\mathrm{A}}^{(ABC)} - E_{\mathrm{B}}^{(ABC)} - E_{\mathrm{C}}^{(ABC)} = V(R) \qquad (2)$$

superposition error (BSSE)[28] on ΔE was thereby performed. The calculations were mostly carried out at MP2 level. The optimized interaction energy $V(R_e)$ and Au–Au (R_e) distances for the dimers and trimers are shown in Table 3. These results were obtained by using the fitting procedure described in the Part 1.[21] We would like to emphasize that the interaction energy is obtained by a supermolecular approach. Another option would have been to use symmetry-adapted perturbation theory.[29]

Table 3. Optimized MP2 Au–Au distances, R_e, for [(XAuL)$_n$] (n = 2, 3). Distance in pm; interaction energy $V(R_e)$ in au.

System	R_e	$V(R_e)$
[(ClAuPH$_3$)$_2$] (C_2)	320.8	–0.009407
[(ClAuPH$_3$)$_2$] (C_{2v})	[a]	
[(ClAuPH$_3$)$_2$] (C_{2h})	384.9	–0.018652
[(ClAuPMe$_3$)$_2$] (C_2)	375.5	–0.008451
[(IAuPH$_3$)$_2$] (C_2)	315.4	–0.012315
[(HAuNCH)$_2$] (C_2)	312.8	–0.005826
[(HAuNCH)$_2$] (C_{2v})	[a]	
[(HAuNCH)$_2$] (C_{2h})	316.4	–0.009239
[(ClAuPH$_3$)$_3$] (perpendicular)	316.9	–0.018802
[(HAuNCH)$_3$] (perpendicular)	308.2	–0.010185
[(HAuNCH)$_3$] (linear)	[a]	
[(HAuNCH)$_3$] (triangle)	[a]	

[a] Repulsive curve; no minimum found.

Theory of Intermolecular Forces: An alternative partitioning of the interaction energies of the Equations (1) and (2) is given in Equation (3), where

$$\Delta E(\mathrm{MP2}) = \Delta E(\mathrm{HF}) + \Delta E^{(2)} \qquad (3)$$

ΔE(HF) is the interaction energy evaluated from a self-consistent field (SCF) supermolecule calculation at Hartree–Fock (HF) level. Because the intramolecular second-order correlation energy is included in E_A, $\Delta E^{(2)}$ is a useful approximation to the dispersion energy at second order of the many-body perturbation treatment (MBPT).[30, 31]

The total intermolecular potential V_{int}[20, 32] can be partitioned into different contributions at long ranges [Eq. (4)],[33, 34] where the overlap between the

$$V_{\mathrm{int}} = V_{\mathrm{short}} + V_{\mathrm{elect}} + V_{\mathrm{ind}} + V_{\mathrm{disp}} \qquad (4)$$

molecular charge clouds is insignificant. The four terms are the short-range (V_{short}), electrostatic (V_{elect}), induction (V_{ind}) and dispersion (V_{disp}) contributions. For a bound system, the intermolecular forces are repulsive at short range and attractive at long distance; there must be at least two contributions of opposite sign to the total force, leading to the appearence of the van der Waals minimum. The repulsive effects at short distance appear because the electron clouds of the monomers penetrate each other and bring about charge overlap and exchange effects. The electrostatic and induction energies are classical long-range contributions. Finally, the dispersion (London) energy also has a long-range character, but requires a quantum mechanical interpretation.[33]

It is common practice to associate the Hartree–Fock term (ΔE(HF)) with the sum of short-range (V_{short}), electrostatic (V_{elect}) and induction (V_{ind}) terms; while the, $\Delta E^{(2)}$ electron correlation term is associated with dispersion (V_{disp}).[34] Hence, we can separate the different attractive or repulsive contributions and their source at long-range for dimers and trimers. Furthermore, if the separation between the monomers is large compared with their dimensions, a multipole moment expansion of the interaction Hamiltonian may be made and the V_{elect} expressed in terms of the permanent multipole moments of each monomer. Hence, our aim is to relate the intermolecular potential to the properties of the isolated molecules through the total charge (q), dipole moment (μ), quadrupole moment (θ), polarizability (α) and first ionization potential (IP_1).[20, 32] These properties are given in the Table 4 for each monomer studied. Both HF and MP2 results are given. The latter are used in the Figures and in Table 5.

The interaction of the dimers [(X-Au-L)$_2$] in their different orientations (parallel (C_{2v}), antiparallel (C_{2h}), and perpendicular (C_2); Figure 1) will be studied using the specific configuration given for two C_{3v} molecules A and B[20] with respect to their dipole moment as shown in the Figure 2. The angles ϑ_A and ϑ_B are fixed at 90°. For this special case, the expressions for the intermolecular potential are outlined in the following sections 1–3.

1) Electrostatic Interactions: The electrostatic energy (V_{elect}) of a pair of molecules (monomers) is the energy of interaction between their permanent

$$V_{\mathrm{elect}} = \frac{3}{4}\frac{\theta^{(A)}\theta^{(B)}}{R^5}(1 + 2\cos^2\phi) + \frac{\mu^{(A)}\mu^{(B)}}{R^3}\cos\phi \qquad (5)$$

Table 4. Finite field calculations of electric properties of [XAuL] monomers at Hartre–Fock (HF) level and the increment due to MP2-level electron correlation (2). All values in au.

Properties	[ClAuPH$_3$]	[ClAuPMe$_3$]	[IAuPH$_3$]	[HAuNCH]
μ(HF)	3.29335	3.85520	3.68506	3.05302
(2)	−0.13068	−0.27105	−0.43896	−0.48164
α(HF)	63.58702	95.23497	85.98593	50.86690
(2)	6.90562	8.35751	8.08540	1.95122
$\alpha_\parallel$(HF)	88.27307	118.37330	125.69640	67.09482
(2)	15.27802	18.45078	20.35960	4.53388
$\alpha_\perp$(HF)	51.24399	83.66580	66.13070	42.75301
(2)	2.71941	3.31089	1.94829	0.65982
θ(HF)	0.65968	7.23505	9.17850	14.80905
(2)	1.95297	−3.58266	0.31842	0.15346
IP_1(HF)	0.38061	0.36686	0.31842	0.31899
(2)	0.00549	0.00000	−0.01127	−0.00165

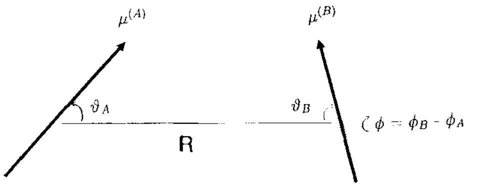

Figure 2. Definition of coordinates for the two polar molecules A and B.

charge distributions [Eq. (5)]. The electrostatic energy is of first order in the Coulomb interaction and as such is pairwise additive. Note that the quadrupole term is always repulsive for A = B. The dipole–quadrupole cross-term vanishes for $\vartheta_A = \vartheta_B = 90°$.

2) Induction Interactions: The induction energy (V_{ind}) results from the interaction of the induced electric moments of each molecule with the permanent charge distribution of its partners. The contribution from monomer B is for the angles $\vartheta_A = \vartheta_B = 90°$ [Eq. (6)], where $\alpha_\parallel$ and $\alpha_\perp$ are parallel and

$$V_{ind}^{(B)} = -\frac{1}{2}\sum_A\left[\frac{\alpha^{(B)}\mu^{(A)2}}{R^6} + \frac{1}{3}\frac{(\alpha_\parallel - \alpha_\perp)^{(B)}}{R^6}\mu^{(A)2}(3\cos^2\phi - 1)\right] \tag{6}$$

perpendicular components, respectively, of the total polarizability α. This term is rarely the dominant source of attraction between molecules and is smaller than the electrostatic and dipersion energies. The induction energy is not pairwise additive.

3) Dispersion (London) Interactions: The dispersion term makes an important contribution to the intermolecular potential and is attractive between polar or nonpolar molecules at long and short distance. If the average excitation energy is approximated by the ionization potential IP_1, which can be obtained from Koopmans's theorem,[35] and static polarizabilities are used, we obtain the London approximation given in Equation (7). The leading

$$V_{disp} = -\frac{4}{3}\frac{IP_1}{R^6}\left(\alpha^2 - \frac{1}{3}\alpha(\alpha_\parallel - \alpha_\perp)\right) \tag{7}$$

dispersion term behaves as $V_{disp} = -C_6/R^6$. The exact expression for the dispersion coefficient C_6 can be obtained from the Casimir–Polder formula [Eq. (8)],[36] where $\alpha_1^A(iE)$ is the dipole polarizability of monomer A, evaluated at imaginary frequency iE. At short range, a cut-off is introduced by the finite molecular size, and the true dispersion energy [unlike Eq. (7)] does not became infinite at $R = 0$. The higher-multipolarity polarizabities $\alpha_L(iE)$ ($L > 1$) lead to the higher-order interaction terms C_8, C_{10}, etc. The dispersion terms (7–8) are additive. The first nonadditive dispersion term is the Axilrod–Teller[37] third-order term.

$$C_6 = \frac{3}{\pi}\int_0^\infty \alpha_1^A(iE)\alpha_1^B(iE)\,dE \tag{8}$$

Non-additive Effects: For complexes composed of more than two monomers, for instance for trimers of type [(X-Au-L)$_3$], one has to account for all pairwise interactions as well as to allow for nonpairwise or nonadditive effects. Although nonadditive effects are in general much smaller than the additive component of the interaction energy (usually by 1 or 2 orders of magnitude), they can be significant when considering the properties of bulk matter and molecular clusters.[33, 22]

The nonadditivity in polar complexes appear in induction, dispersion and exchange energies. In general, for complexes of polar molecules, the three-body interaction is dominated by the induction nonadditive effects.[38, 39] The dispersion effect is usually much smaller. The overall three-body interaction is thus well approximated at the Hartree–Fock (HF) level.

We study the nonadditive effects for trimers [(X-Au-L)$_3$] in different orientations (perpendicular, linear and triangular) (Figure 3) by means of the deviation from pairwise additivity (ΔX),[40] which is obtained as the difference between the interaction energy of the trimer and all pairwise interaction energies of dimers [Eq. (9)]. We have derived for the trimers in Figure 3 some expressions for three-body and pairwise induction. First, the local electric field at site i is obtained as Equation (10). Then, the expression

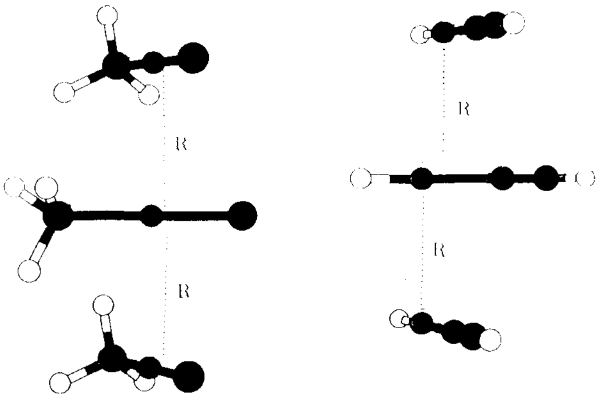

(a) Linear Perpendicular (b) Linear Perpendicular

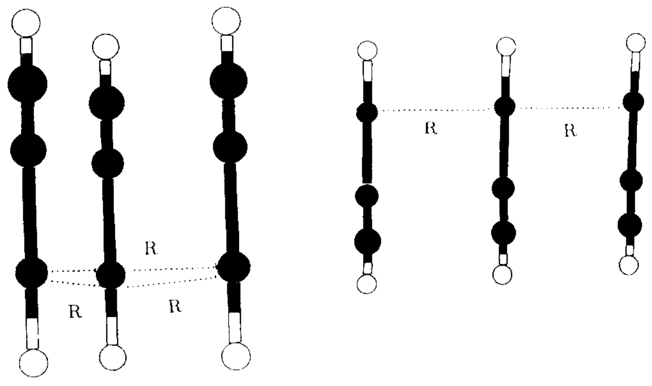

(c) Equilateral Triangle (d) Linear Parallel

Figure 3. a,b) Linear perpendicular, c) triangular and d) linear parallel orientations of trimers [(XAuL)$_3$].

$$\Delta X = \Delta E(\text{trimer}) - \sum_{\text{all pair}} \Delta E(\text{pairwise}) \tag{9}$$

$$E_i = \sum_j E_{ij} \tag{10}$$

for the total interaction energy W becomes Equation (11), where W_i is given by Equation (12). Here, E_i is the total electric field at site i. The three-body interaction is obtained by subtracting from W the sum of the pairwise interactions. For identical monomers, the following special cases were studied:

$$W = \sum_i W_i \tag{11}$$

$$W_i = -\frac{1}{2} E_i \alpha E_i \tag{12}$$

1) *Linear perpendicular orientation* [Eq. (13) and (14)]:

$$V^{\text{ind}}_{\text{pairwise}} = -\frac{\mu^2}{R^6}\left[2\alpha_{\perp} + \frac{\alpha_{\parallel}}{64}\right] \tag{13}$$

$$V^{\text{ind}}_{\text{three-body}} = -\frac{\mu^2}{R^6}\left[\alpha_{\perp} + \frac{\alpha_{\parallel}}{4}\right] \tag{14}$$

2) *Linear parallel orientation* [Eq. (15) and (16)]:

$$V^{\text{ind}}_{\text{pairwise}} = -\frac{\mu^2\alpha_{\parallel}}{R^6}\left[\frac{129}{64}\right] \tag{15}$$

$$V^{\text{ind}}_{\text{three body}} = -\frac{\mu^2\alpha_{\parallel}}{R^6}\left[\frac{5}{4}\right] \tag{16}$$

3) *Equilateral triangle* [Eq. (17)]:

$$V^{\text{ind}}_{\text{pairwise}} = V^{\text{ind}}_{\text{three-body}} = -\frac{3\mu^2\alpha_{\parallel}}{R^6} \tag{17}$$

These expressions can be used for understanding the source of the deviation from additivity in the trimers at MP2 and Hartree–Fock levels. As a general comment, at large R, the comparison between numerical results and theoretical expressions is limited by numerical noise. At small R the multipole expansion (including the choice of origin, not necessarily at the gold atom) will break down.

Results and Discussion

Perpendicular (C_2) Orientation in Dimers [(XAuL)$_2$]:

The [(XAuPR$_3$)$_2$] systems: We consider first the dimer [(ClAuPH$_3$)$_2$], and then its results are generalized for [(ClAuPMe$_3$)$_2$] and [(IAuPH$_3$)$_2$]. The intermolecular interaction energy at MP2 level for the dimer [(ClAuPH$_3$)$_2$] is shown in Figure 4. An energy minimum occurs at $R_e = 320.8$ pm. Obviously, at this distance the attractive and repulsive dV/dR terms cancel. The main repulsive term, the Pauli repulsion, already occurs at HF level. Note that the total MP2 curve lies below the $\Delta E^{(2)}$ curve near R_e, but above it for large R. The difference (i.e. the HF contribution) is dominated by the repulsive Pauli term and the attractive induction term in the two cases, respectively.

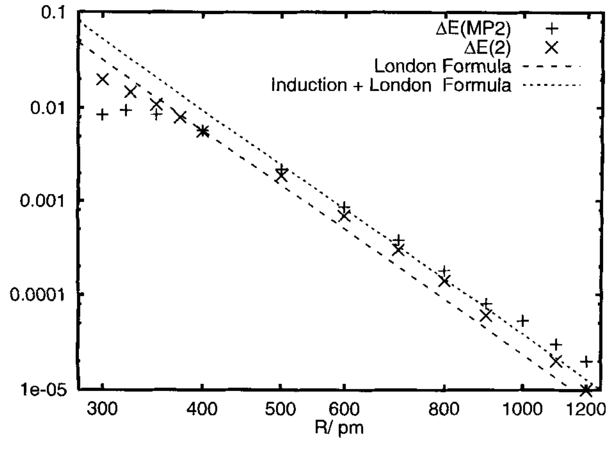

Figure 4. Interaction energy, $V(R)$, in the perpendicular (C_2) orientation of the dimer [(ClAuPH$_3$)$_2$].

The long-range behaviour can be compared with the sum of the two R^{-6} attractive terms from induction and dispersion, estimated with Equations (6) and (7), respectively. The agreement is reasonable. *The extrapolation from large R to R_e forms our best proof that the dispersion term is the main contribution to the aurophilic attraction.* The electrostatic dipole–dipole interaction vanishes at $\phi = 90°$. The quadrupole–quadrupole term is small and repulsive.

The corresponding curves for [(ClAuPMe$_3$)$_2$] and [(IAuPH$_3$)$_2$] are shown in Figures 5 and 6, respectively. The effective C_6 coefficients are shown in Table 5.

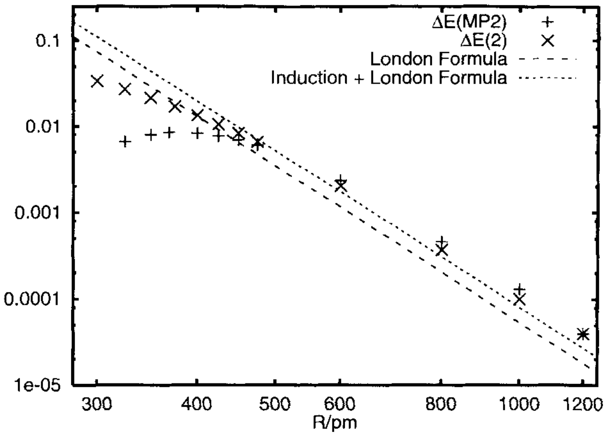

Figure 5. Interaction energy, $V(R)$, in the perpendicular (C_2) orientation of the dimer [(ClAuPMe$_3$)$_2$].

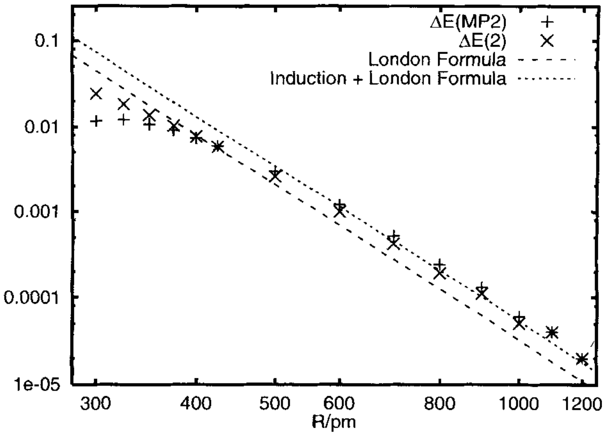

Figure 6. Interaction energy, $V(R)$, in the perpendicular (C_2) orientation of the dimer [(IAuPH$_3$)$_2$].

Table 5. Dispersion coefficients C_6 (in 10^{12} au pm^{-6}) for the perpendicular (C_2) geometry of dimer [(XAuL)$_2$]. MP2-level monomer properties are used for the London and induction components.

System	$\Delta E^{(2)}$	MP2	London	London + Induction
[(ClAuPH$_3$)$_2$]	35.2	40.1	23.5	38.5
[(ClAuPMe$_3$)$_2$]	94.6	112.4	53.2	80.6
[(IAuPH$_3$)$_2$]	48.2	56.5	32.4	53.3
[(HAuNCH)$_2$]	18.2	8.7	12.8	22.4

The [(HAuNCH)$_2$] systems: This system yields different results from those described above (Figures 7 and 8). At short distances this system shows an attractive $V(R)$ curve, like the earlier three perpendicular dimers. The second order $\Delta E^{(2)}$ contribution to the total interaction energy (ΔE(MP2)) behaves as R^{-6} at large R and agrees with the London formula. However, the interaction energy at long distance (above 500 pm) is dominated by the Hartree–Fock term (HF) (see Figure 8). This term behaves as R^{-5}, and is quite close to the quadrupole–quadrupole contribution from the electrostatic formula [Eq. (5)].

Near the minimum, between 300 and 400 pm, the quadrupole–quadrupole repulsion is weakened by the induction terms (already present at HF level, see Figure 8), and cancelled entirely by the correlation term $\Delta E^{(2)}$ (see Figure 7).

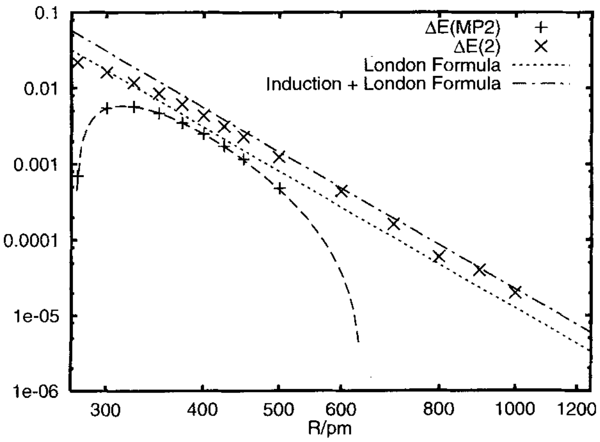

Figure 7. The attractive contributions to $V(R)$ in the perpendicular orientation of the dimer [(HAuNCH)$_2$].

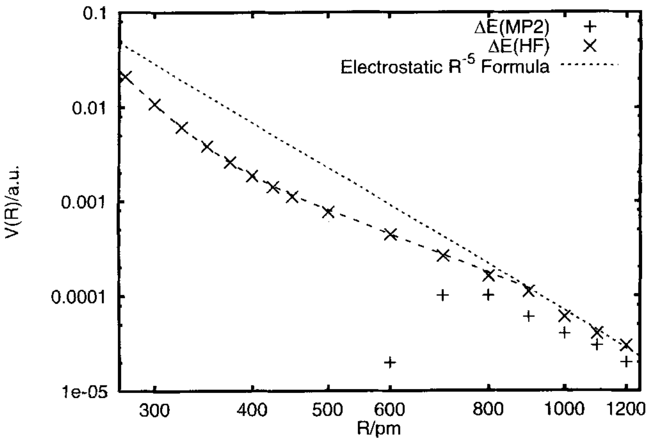

Figure 8. The repulsive contributions to $V(R)$ in the perpendicular orientation of the dimer [(HAuNCH)$_2$].

As seen from Table 4, HAuNCH is unique in having the smallest α and the largest θ among the four monomers. This explains why the electrostatic term overrides the dispersion term above $R = 600$ pm.

Parallel (C_{2v}) and Antiparallel (C_{2h}) Orientation in Dimers [(XAuL)$_2$]: In this section, we will examine the dominant mechanisms at work in the parallel and antiparallel orientations of the dimers [(ClAuPH$_3$)$_2$] and [(HAuNCH)$_2$].

The [(ClAuPH$_3$)$_2$] system: The results for the antiparallel orientation (C_{2h}) are shown in Figure 9. The total interaction energy at MP2 level (ΔE(MP2)) reaches a minimum around 375 pm. The Hartree–Fock (HF) term is attractive and produces a minimum at 400 pm. At MP2 level, the attraction is strengthened and R_e shortened, to 385 pm (see Table 3). Thus the dispersion in not negligible, even in this dipole-dominated case. For long distances (above 400 pm), the HF term dominates. It shows quite a close relationship with the dipole–dipole R^{-3} formula. The repulsive quadrupole–quadrupole term is not important.

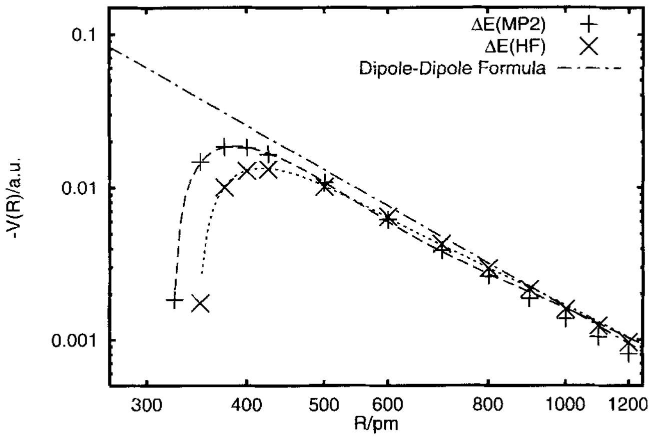

Figure 9. Interaction energy in the antiparallel (C_{2h}) orientation of the dimer [(ClAuPH$_3$)$_2$].

The parallel orientation (C_{2v}) (Figure 10) is dominated by dipole–dipole repulsion at both HF and MP2 level. The calculated HF curve goes over to the dipole limit at large R. The MP2 curve develops a bulge, but remains repulsive.

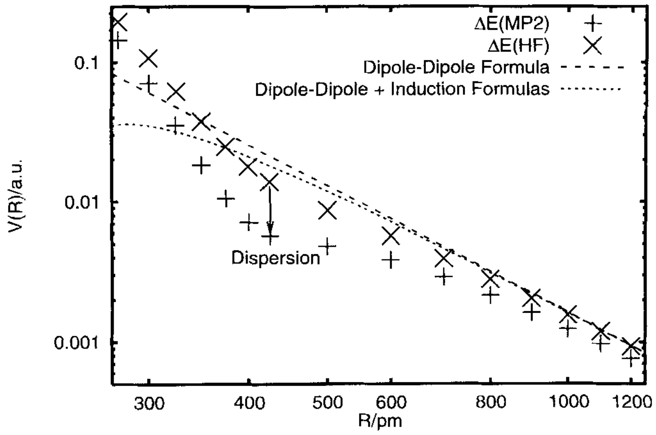

Figure 10. Long-range limit in the parallel (C_{2v}) orientation of the dimer [(ClAuPH$_3$)$_2$].

Thus, both orientations are dominated by the electrostatic dipole–dipole interaction, but, even here, the correlation effects are not negligible (as already suggested by Pyykkö and Zhao[31]).

The [(HAuNCH)$_2$] system: Figure 11 shows the results for the antiparallel orientation (C_{2h}). At long range, the attractive electrostatic dipole–dipole R^{-3} term is partially cancelled by the

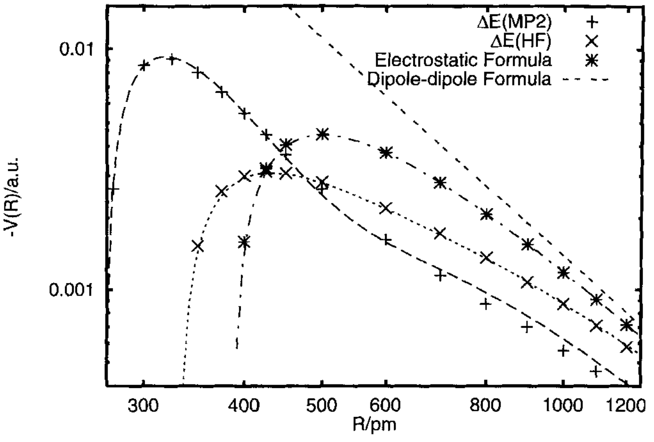

Figure 11. Long-range limit in the antiparallel (C_{2h}) orientation of the dimer [(HAuNCH)$_2$].

repulsive R^{-5} quadrupole–quadrupole term. Their sum is not far from the HF curve. At short distances the correlation effects become predominant, overtaking the quadrupole–quadrupole repulsion, and lead to a minimum near 316 pm.

For the parallel orientation (C_{2v}), the interaction energy at MP2 level (Figure 12) is repulsive at all distances, but there is a local minimum at 350 pm. At short distance, the $\Delta E^{(2)}$ is important, and produces the minimum at MP2 level. The HF curve is repulsive; the dipole–dipole repulsion is now strengthened by the quadrupole–quadrupole term. The downwards deviation of the HF curve from the electrostatic curve at around 400 pm can be ascribed to induction.

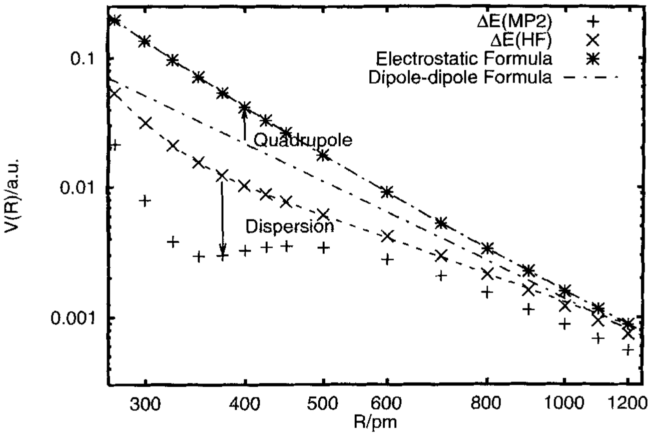

Figure 12. Long-range limit in the parallel (C_{2v}) orientation of the dimer [(HAuNCH)$_2$].

We conclude that, for this specific system, which has the largest quadrupole moment θ, the quadrupole, induction and dispersion terms remain relevant, even at geometries permitting maximum dipole contributions.

Trimers [(XAuL)$_3$]; Nonadditive Effects: We now examine the nonadditive effects in the trimers [(XAuL)$_3$] for different orientations (see Figure 3). The nonadditivity is described through the deviation from pairwise additivity [ΔX of Eq. (9)] at MP2 level. Moreover, we analyse the results by partitioning the deviation ΔX(MP2) into Hartree–Fock (ΔX(HF)) and electron correlation (ΔX(2)) contributions, respectively. The ΔX(HF) contribution is analysed by means of the pairwise and three-body induction formulae [Eq. (13)–(17)] for each specific orientation of the trimers.

Perpendicular orientation in [(ClAuPH$_3$)$_3$] and [(HAuNCH)$_3$]: For both trimers, we obtained an attractive intermolecular interaction energy, with gold–gold distances and energies of comparable magnitude to those of the dimers (see Table 3).

The results of the deviation from pairwise additivity (ΔX) are shown in Figures 13 and 14 for [(ClAuPH$_3$)$_3$] and [(HAuNCH)$_3$], respectively. The deviation of electron correlation ΔX(2) (not included) is very small; thus, the ΔX(HF) contribution dominates at long distances (above 400 pm) and is the main source of the deviation.

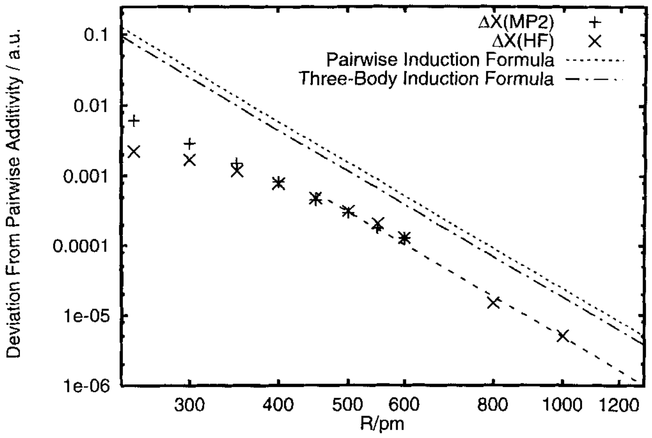

Figure 13. Nonadditivity in perpendicular trimer [(ClAuPH$_3$)$_3$].

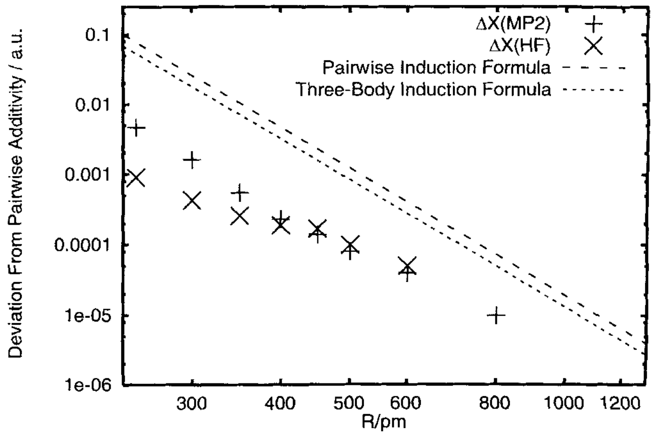

Figure 14. Nonadditivity in perpendicular trimer [(HAuNCH)$_3$].

For the trimer [(ClAuPH$_3$)$_3$], the deviation ΔX(HF) behaves as R^{-6}, similarly to the three-body and pairwise induction formulae [Eq. (13) and (14)] between 400 and 1000 pm (see Figure 13). This situation is also found for the trimer [(HAuNCH)$_3$] (Figure 14), but it does not show a close correlation with the induction formulae.

Parallel linear and triangular orientations in trimer [(HAuNCH)$_3$]: For both orientations in the trimer [(HAuNCH)$_3$], we obtained an intermolecular interaction energy which is repulsive at MP2 level.

The results of the deviation from pairwise additivity (ΔX) are shown in the Figure 15 and 16 for linear and triangular geometries, respectively. The ΔX(HF) contribution dominates at long distance and is the main source of the deviation. For the triangular geometry, it shows a quite close relationship with the deviation ΔX(MP2) at all distances (see Figure 16).

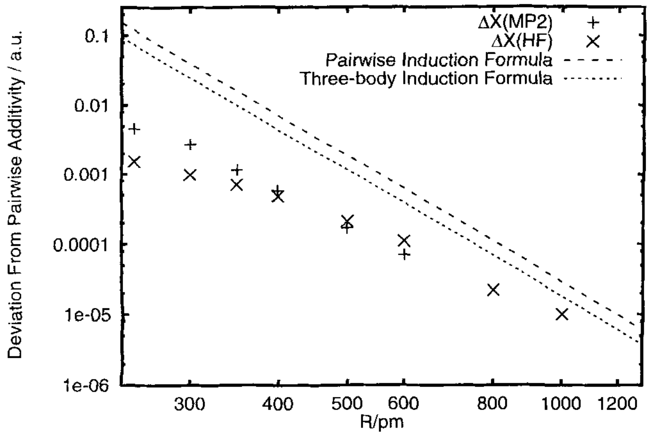

Figure 15. Nonadditivity in parallel linear trimer [(HAuNCH)$_3$].

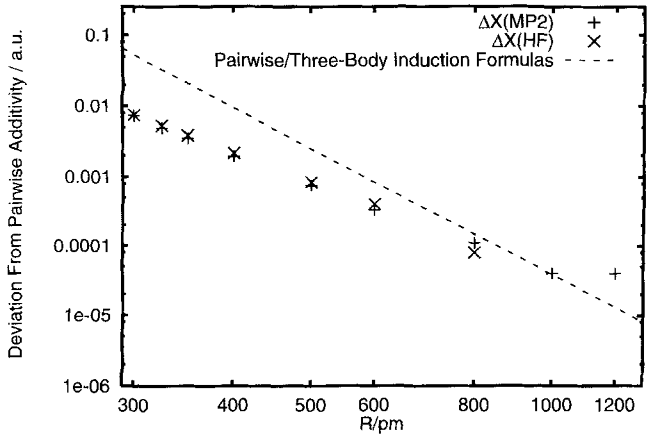

Figure 16. Nonadditivity in triangular trimer [(HAuNCH)$_3$].

The deviation ΔX(HF) for both orientations shows similar results when we compared it with the pairwise and three-body induction formulae [Eq. (15)–(17)]. The R^{-6} long-range behaviour was verified.

Through this analysis, we have found the nature of the nonadditive effects already at the Hartree–Fock level. The agreement with the induction formulae for the trimers [(ClAuPH$_3$)$_3$] and [(HAuNCH)$_3$] at large distance is acceptable .

Conclusions

We have analysed the intermolecular interaction energy in dimers and trimers of various [X-Au-L] systems as a function of the Au–Au distances R. The dominant terms at various distances are related to the properties of the monomers. The main conclusions are:

1) The model systems [(XAuPR$_3$)$_2$] (X = Cl, I and R = H, Me) with perpendicular (C_2) orientations are found to give similar results. The R^{-6} behaviour at large distances provides the best proof so far for the dispersive character of the aurophilic attraction.
2) The pairwise induction contributions to C_6 are, however, not negligible.
3) The model system [(HAuNCH)$_2$] with a perpendicular (C_2) orientation is dominated at large distances by the repulsive, quadrupole–quadrupole term, owing to the large quadrupole moment of that monomer.
4) For the [(ClAuPH$_3$)$_2$] system with parallel (C_{2v}) and antiparallel (C_{2h}) orientations, the R^{-3} dipole–dipole term dominates at long distances, while the correlation effects become important at intermediate distances.
5) For the [(HAuNCH)$_2$] system, both the R^{-3} dipole and the R^{-5} quadrupole terms are important. At intermediate distances the correlation term is comparable with that of the other dimers.
6) For the first time we point out the possibility of nonadditive induction terms becoming particularly important for large oligomers with several Au$^{\text{I}}$ centres.

Acknowledgment: P. Pyykkö thanks The Academy of Finland (FA) for a Research Professorship from August 1995 to July 2000. F. M. is also supported by FA. DEC Alpha Stations of our laboratory and computer resources from the Center for Scientific Computing (CSC), Espoo, were used in this research.

Received: January 21, 1997 [F596]

[1] H. Schmidbaur, *Gold Bull.* **1990**, *23*, 11.
[2] H. Schmidbaur, *Chem. Soc. Rev.* **1995**, 391.
[3] P. Pyykkö, Y.-F. Zhao, *Angew. Chem.* **1991**, *103*, 622; *Angew. Chem. Int. Ed. Engl.* **1991**, *30*, 604.
[4] P. Pyykkö, J. Li, N. Runeberg, *Chem. Phys. Lett.* **1994**, *218*, 133.
[5] P. Pyykkö, *Chem. Rev.* **1997**, *97*, 597.
[6] I. Dance in *The Crystal as a Supramolecular Entity* (Ed.: G. R. Desiraju), Wiley, Chichester, **1995**, pp. 137–233.
[7] A. Bauer, A. Schier, H. Schmidbaur, *J. Chem. Soc. Dalton Trans.* **1995**, 2919.
[8] D. M. P. Mingos, J. Yau, S. Menzer, D. J. Williams, *J. Chem. Soc. Dalton Trans.* **1995**, 319.
[9] H. Xiao, K.-K. Cheung, C.-M. Che, *J. Chem. Soc. Dalton Trans.* **1996**, 3699.
[10] W. Schneider, K. Angermaier, A. Sladek, H. Schmidbaur, *Z. Naturforsch.* **1996**, *51b*, 790.
[11] A. Sladek, K. Angermaier, H. Schmidbaur, *Chem. Commun.* **1996**, 1959.
[12] D. Perreault, M. Drouin, A. Michel, V. M. Miskowski, W. P. Schaefer, P. D. Harvey, *Inorg. Chem.* **1992**, *31*, 695.
[13] K. Angermair, G. A. Bowmaker, E. N. de Silva, P. C. Healy, B. E. Jones, H. Schmidbaur, *J. Chem. Soc. Dalton Trans.* **1996**, 3121.
[14] H. Schmidbaur, W. Graf, G. Müller, *Angew. Chem.* **1988**, *100*, 439; *Angew. Chem. Int. Ed. Engl.* **1988**, *27*, 417.
[15] R. Narayanaswamy, M. A. Young, E. Parkhurst, M. Ouellette, M. E. Kerr, D. M. Ho, R. C. Elder, A. E. Bruce, M. R. M. Bruce, *Inorg. Chem.* **1993**, *32*, 2506.
[16] A. Dedieu, R. Hoffmann, *J. Am. Chem. Soc.* **1978**, *100*, 2074.
[17] Y. Jiang, S. Alvarez, R. Hoffmann, *Inorg. Chem.* **1985**, *24*, 749.
[18] J. Li, P. Pyykkö, *Chem. Phys. Lett.* **1992**, *197*, 586.
[19] P. Pyykkö, K. Angermaier, B. Assmann, H. Schmidbaur, *J. Chem. Soc. Chem. Commun.* **1995**, 1889.
[20] A. D. Buckingham in *Intermolecular Forces: From Diatomics to Biopolymers* (Ed. B. Pullman), Wiley, New York, **1978**, pp. 1–67.
[21] P. Pyykkö, N. Runeberg, F. Mendizabal, *Chem. Eur. J.* **1997**, 3, 1451.
[22] G. Chalasiński, M. M. Szcześniak, *Chem. Rev.* **1994**, *94*, 1723.
[23] M. J. Frisch, G. W. Trucks, H. B. Schlegel, P. M. W. Gill, B. G. Johnson, M. A. Robb, J. R. Cheeseman, T. A. Keith, G. A. Petersson, J. A. Montgomery, K. Raghavachari, M. A. Al-Laham, V. G. Zakrzewski, J. V. Ortiz, J. B. Foresman, J. Cioslowski, B. B. Stefanov, A. Nanayakkara, M. Challacombe, C. Y. Peng, P. Y. Ayala, W.Chen, M. W. Wong, J. L. Andres, E. S. Replogle, R. Gomperts,

R. L. Martin, D. J. Fox, J. S. Binkley, D. J. Defrees, J. Baker, J. P. Stewart, M. Head-Gordon, C. Gonzalez, and J. A. Pople, Gaussian, Inc., Pittsburgh PA, 1995.
[24] D. Andrae, U. Häusserman, M. Dolg, H. Stoll, H. Preuss, *Theor. Chim. Acta* **1990**, *77*, 123.
[25] A. Bergner, M. Dolg, W. Küchle, H. Stoll, H. Preuss, *Mol. Phys.* **1993**, *80*, 1431.
[26] S. Huzinaga, *Gaussian Basis Sets for Molecular Calculations*, Elsevier, Amsterdam, **1984**, p. 16.
[27] T. H. Dunning, Jr., P. J. Hay in *Modern Theoretical Chemistry, Vol. 3* (Ed.: H. F. Schaefer III), Plenum Press, New York, **1977**, pp. 1–28.
[28] S. F. Boys, F. Bernardi, *Mol. Phys.* **1970**, *19*, 553.
[29] B. Jeziorski, R. Moszynski, K. Szalewicz, *Chem. Rev.* **1994**, *94*, 1887.
[30] C. Møller, M. S. Plesset, *Phys. Rev.* **1934**, *46*, 618.
[31] P. Hobza, R. Zahradnik, *Chem. Rev.* **1988**, *88*, 871.
[32] J. A. Pople, *Faraday Discuss. Chem. Soc.* **1982**, *73*, 7.
[33] G. Chalasiński, M. Gutowski, *Chem. Rev.* **1988**, *88*, 943.
[34] A. D. Buckingham, P. W. Fowler, J. M. Hutson, *Chem. Rev.* **1988**, *88*, 963.
[35] T. A. Koopmans, *Physica* **1933**, *1*, 104.
[36] H. B. G. Casimir, D. Polder, *Phys. Rev.* **1948**, *73*, 360.
[37] B. M. Axilrod, E. Teller, *J. Chem. Phys.*, **1943**, *11*, 299.
[38] G. Chalasiński, S. M. Cybulski, M. M. Szcześniak, S. J. Scheiner, *J. Chem. Phys.* **1989**, *91*, 7048.
[39] M. M. Szcześniak, R. A. Kendall, G. Chalasiński, *J. Chem. Phys.* **1991**, *95*, 5169.
[40] R. F. W. Bader, O. A. Novaro, V. Beltrán-Lopéz, *Chem. Phys. Letters* **1971**, *8*, 558.